16th July 2015

Intrinsically Microporous Polymer Slows Down Fuel Cell Catalyst Corrosion

Daping He [1,2], Yuanyang Rong [1], Zongkui Kou [2], Shichun Mu [2], Tao Peng [3], Richard Malpass-Evans [4], Mariolino Carta [4], Neil B. McKeown [4], and Frank Marken*[1]

[1] Department of Chemistry, University of Bath, Claverton Down, Bath BA2 7AY, UK
[2] State Key Laboratory of Advanced Technology for Materials Synthesis and Processing, Wuhan University of Technology, Wuhan 430070, China
[3] Department of Civil and Environmental Engineering, University of Windsor, Sunset Avenue, Ontario, N9B 3P4, Canada
[4] School of Chemistry, University of Edinburgh, David Brewster Road, Edinburgh, EH9 3FJ, UK

To be submitted to Electrochemistry Communications

Proofs to F. Marken (f.marken@bath.ac.uk)

Abstract

The limited stability of fuel cell cathode catalysts causes a significant loss of operational cell voltage with commercial Pt-based catalysts, which hinders the wider commercialization of fuel cell technologies. We demonstrate beneficial effects of a highly rigid and porous polymer of intrinsic microporosity (PIM-EA-TB with BET surface area 1027 m^2 g^{-1}) in accelerated catalyst corrosion experiments. Porous films of PIM-EA-TB offer an effective protective matrix for the prevention of Pt/C catalyst corrosion without impeding flux of reagents. The results of electrochemical cycling tests show that the PIM-EA-TB protected Pt/C (denoted here as PIM@Pt/C) exhibit a significantly enhanced durability as compared to a conventional Pt/C catalyst.

Keywords: Electrocatalysis; Fuel cells; Membrane; Stabilization; Corrosion

Graphical Abstract:

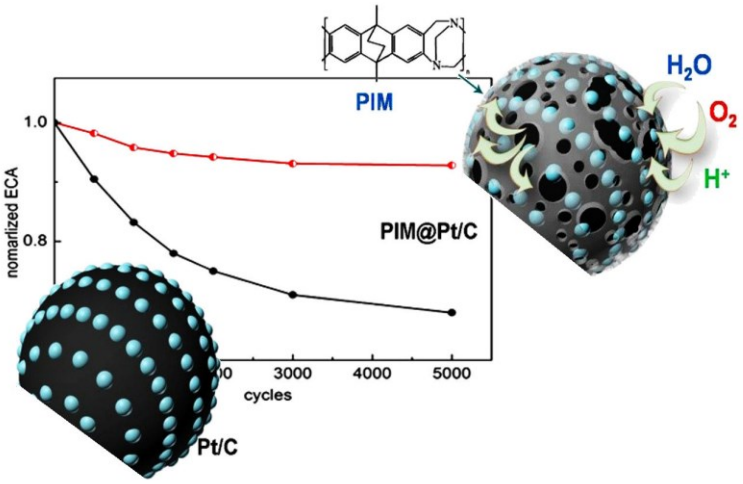

1. Introduction

Polymer electrolyte fuel cells have been extensively investigated as ideal energy sources for portable electronic devices and for electric vehicles due to their high power density and use of environmentally friendly fuels [1,2,3]. However, the expensive metal catalyst Pt, supported on carbon black (here using as the most common electrocatalyst (Pt/C) with 40% Pt on Vulcan 72 [4]) during operation suffers from Pt dissolution [5], Ostwald ripening [6], nanoparticle mobility and aggregation [7], and carbon support electrochemical corrosion [8] in the harsh working environment within polymer electrolyte fuel cells. This commonly leads to a rapid and significant loss of electrochemical surface area [9] (ECA). This drawback, and the problem of slow kinetics of oxygen reduction reaction (ORR) at fuel cell cathodes, still severely hamper the commercialization of fuel cell technology [10,11].

Porous materials such as zirconia [12], silica [13], or tin oxide [14] were supposed to inhibit the migration of metal nanoparticles on catalyst supports. The porous support structure is an attractive way to enhance the stability of metal nanoparticles without effecting the transport of reactants and products. However, with inorganic materials there is still a challenge in precisely controlling the thickness of porous overlayers, and avoiding decrease in catalytic activity. Recently, a novel class of microporous organic materials, polymers with intrinsic microporosity (PIM), has been developed. There are a range of potential applications in gas membrane technology [15,16], in electrolyte media as ionic diode [17], and in electrochemical technology [18,19]. The structurally highly rigid PIM backbone achieves open packing to generate novel properties due to permanent microporosity with ion permeability or semipermeability.

In this study, we exploit a highly porous polymer of intrinsic microporosity (PIM-EA-TB with BET surface area 1027 $m^2 g^{-1}$) as a protection agent for commercial fuel cell catalyst (Pt/C catalyst with 40% Pt on Vulcan-72). Figure 1 schematically shows PIM-EA-TB acting as a stabilizer for the Pt/C catalyst particles.

2. Experimental

2.1. Chemical Reagents

Commercial Pt/C (40 wt. % on Vulcan-72) catalyst and Nafion (5 wt. %) were obtained from Johnson Matthey and Sigma-Aldrich, respectively. Isopropanol, chloroform and perchloric acid (70%–72%), were purchased from Aldrich. PIM-EA-TB was prepared following a literature recipe [20]. Solutions were prepared with filtered and deionized water of resistivity 18.2 MΩ cm from a Thermo Scientific water purification system (ELGA).

2.2. Instrumentation

Electrochemical measurements were performed with a μAutolab III system in a conventional three electrode cell with KCl-saturated calomel (SCE) reference (which is 0.241 V vs. NHE) and platinum wire counter. A Pine AFMSRCE electrode rotator was used for rotating disk electrode (RDE) experiments. Morphologies of the prepared catalysts were analyzed with a JEOL FESEM6301F scanning electron microscope (SEM) and a JEOL 2010 high-resolution transmission electron microscope (HRTEM). TEM samples before and after accelerated degradation testing wer prepared by ultrasonically dispersing

catalyst from the glassy carbon electrode surface into 2 cm^3 ethanol. A volume of 5 μL of the resulting dispersion was the deposited onto an amorphous carbon/Cu grid. XRD spectra were obtained on X-ray diffraction (XRD Bruker D8 ADVANCE, Madison, WI, USA) with a mono-chromatized source of Cu-Kα radiation.

2.3. Procedures for electrode preparation

2 mg of Pt/C catalyst and 100 μL of 5 wt. % Nafion solution were dispersed in 1 mL of isopropanol, followed by a sonication for 15 min to form a homogeneous catalyst ink. 8 μL of the ink was loaded onto a glassy carbon (GC) disk electrode with a diameter of 6 mm. The catalyst layer was allowed to dry under ambient conditions before electrochemical measurement. Coatings with PIM-EA-TB on Pt/C to give PIM@Pt/C were applied as follows: a solution of 1 mg mL^{-1} PIM-EA-TB (10 μL) in chloroform was applied directly onto the Pt/C catalyst layer followed by drying under ambient conditions.

3. Results and Discussion

3.1. Physical Characterisation

Figure 1a shows TEM images of Pt/C catalyst with a size range of 3 to 5 nm for Pt nanoparticles supported on carbon black. The XRD pattern of Pt/C and PIM@Pt/C are shown in Figure 1b. The peaks between 20° and 90° are indexed to Pt crystals of face-centered cubic (fcc) structure. The peaks at 2θ = 39.70°, 46.46°, 67.70°, and 81.42° are assigned to the (111), (200), (220), and (311) planes of Pt, respectively. The presence of PIM did not affect the Pt/C catalyst. Figures 1c,d show SEM images of Pt/C and PIM@Pt/C

catalysts on glassy carbon electrode surfaces. It can be seen that a PIM-EA-TB membrane layer is distributed over the catalyst layer surface.

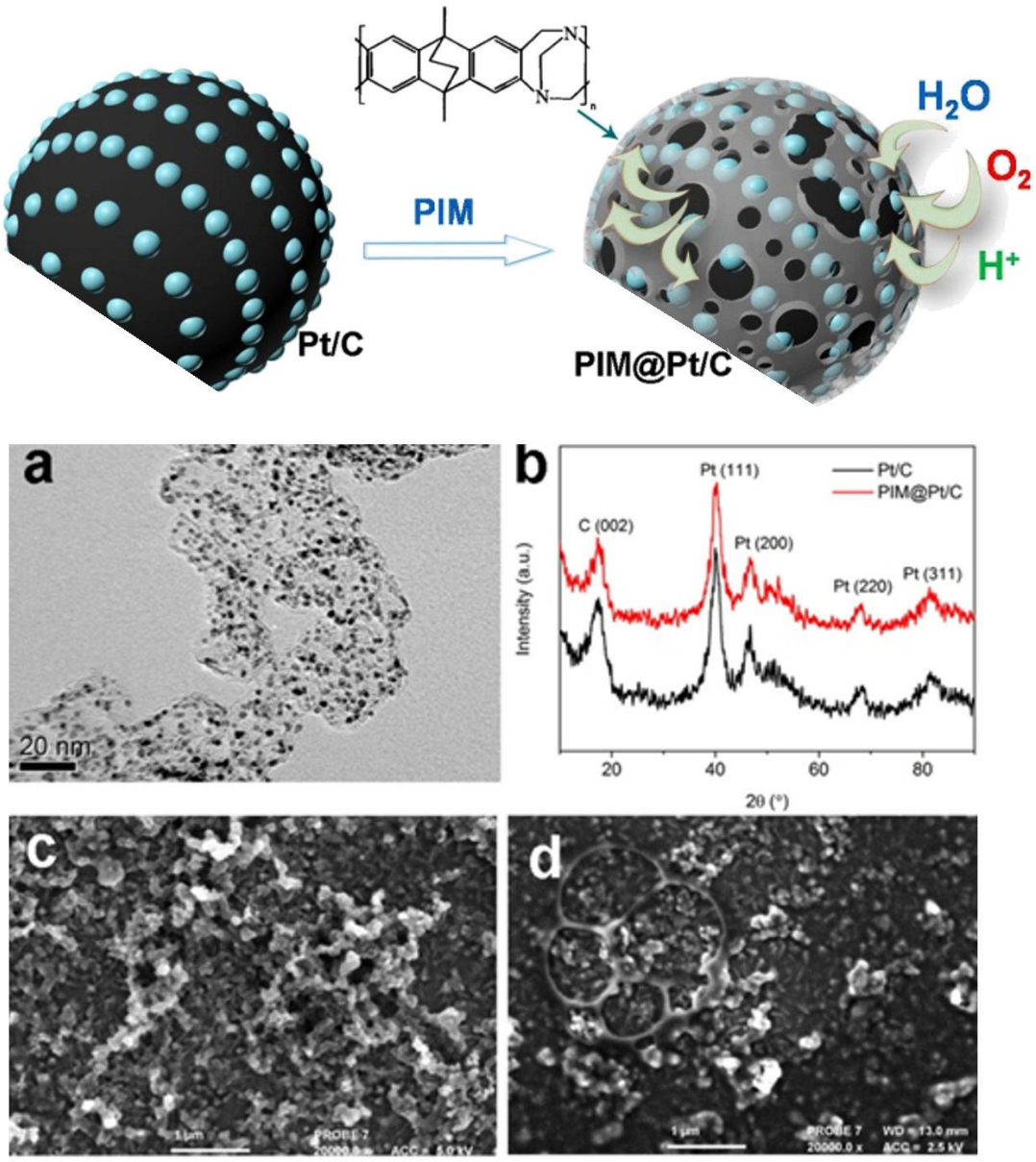

Figure 1. Schematic illustration of Pt/C catalyst protection by PIM-EA-TB. (a) TEM image of Pt/C catalyst. (b) XRD patterns of Pt/C and PIM@Pt/C. SEM images of (c) Pt/C and (d) PIM@Pt/C on glassy carbon electrodes.

3.2. Electrochemical Characterization of Activity and Durability

Figure 2a shows cyclic voltammetry data for the Pt/C and for PIM@Pt/C catalysts recorded in de-aerated 0.1 M $HClO_4$ at room temperature. The electrochemical surface area (ECA) was calculated from the charge under the hydrogen adsorption / desorption region with double-layer charging correction and assuming a value of 210 μC cm^{-2} for the adsorption of a hydrogen monolayer [21]. The PIM@Pt/C catalyst exhibits a very similar electrochemically active surface area (52.6 m^2 g^{-1}) compared to Pt/C (53.7m^2 g^{-1}). Very similar polarization curves for the oxygen reduction reaction in O_2-saturated 0.1 M $HClO_4$ on both catalysts are shown in Figure 2b.

PIM@Pt/C and Pt/C catalysts were then investigated by accelerated degradation testing over 5000 electrochemical oxidation cycles (Figure 2c,d). During potential cycling between 0.541 and 0.941 V at a scan rate of 100 mV s^{-1} in aqueous O_2-saturated $HClO_4$ solution, continuous oxidation and reduction of Pt accelerates the transformation and agglomeration of Pt. As shown Figure 2c, the commercial Pt/C catalyst showed a 54 mV degradation in half-wave potential after 5000 cycles, while the PIM@Pt/C showed only a 7 mV degradation under the same accelerated corrosion condition (see Figure 2d). After 5000 cycles, only 66% of the initial ECA of the Pt/C remains (35.4 m^2 g^{-1}), while 92% of the initial ECA remains for the PIM@Pt/C (48.4 m^2 g^{-1}). The kinetic current was calculated from the ORR polarization curve according to the Koutecky-Levich equation [22]. The ORR kinetic mass activities (at 0.841 V vs. SCE) before and after accelerated corrosion testing are shown in Figure 2f. The initial mass activities for PIM@Pt/C and Pt/C are 40.6

and 41.5 A g^{-1} Pt, respectively, which are then decreased to 28.4 A g^{-1} Pt (70% retention) and 11.6 A g^{-1} Pt (28% retention), respectively. These results indicates a significantly improved stability for PIM@Pt/C.

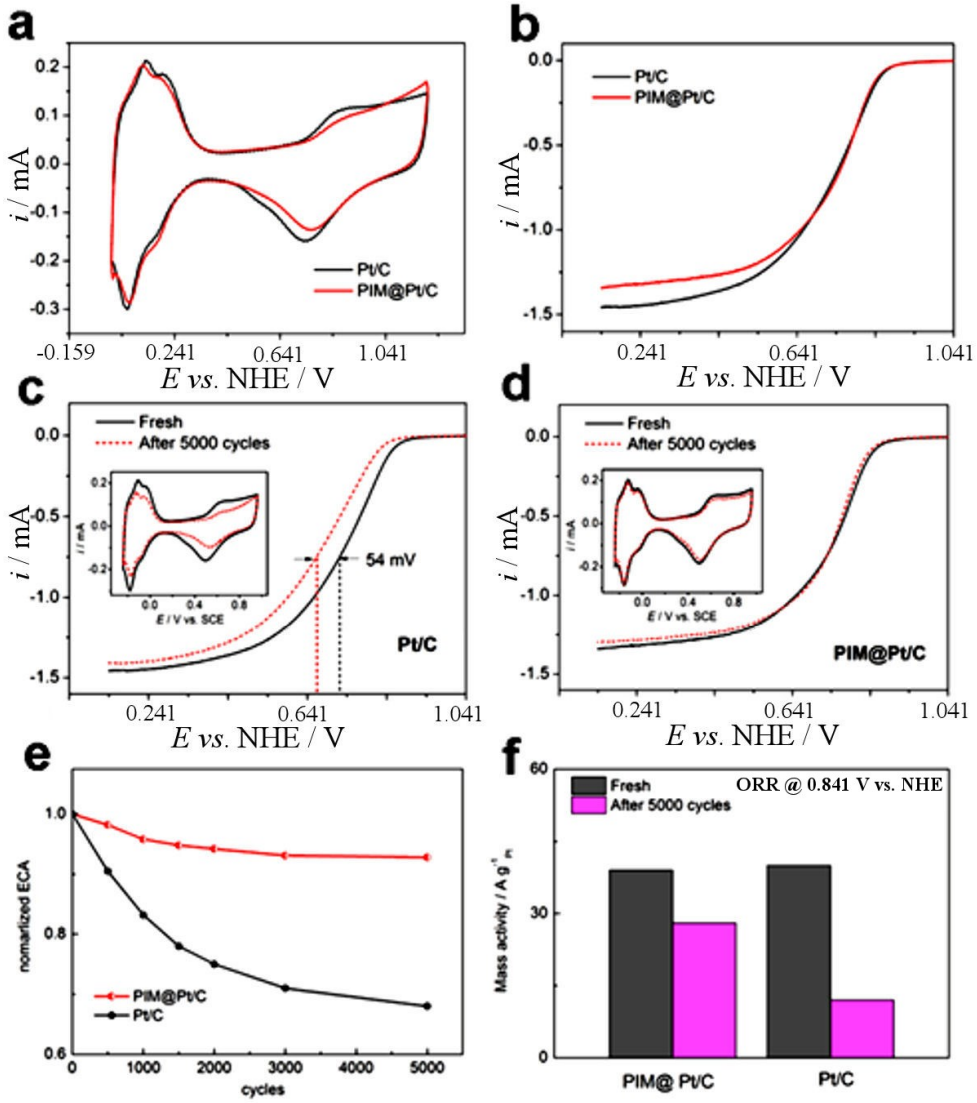

Figure 2. (a) CV curves in N_2-saturated 0.1 M $HClO_4$ (50 mV s^{-1}) and (b) ORR polarization curves in O_2-saturated 0.1 M $HClO_4$ (10 mV s^{-1}, 1600 rpm) for Pt/C and PIM@Pt/C. ORR polarization curves and (inset) CV curves for (c) Pt/C and (d) PIM@Pt/NCWG before and after ADT test cycling from 0.541 to 0.941 V vs. NHE. (e) ECA loss rate and (f) ORR kinetic currents after 5000 cycles ADT test.

Figure 3a-f show the ECA and ORR activity changes for PIM@Pt/C and Pt/C after 4000 cycles testing with the potential range between 0.541 and 1.141 V. Both catalysts show a faster rate of deterioration compared to the previous 0.541-0.941 V test due to the higher over-potential. The activity curves for PIM@Pt/C (Figure 3c,d) decrease more slowly than those for Pt/C (Figure 3a,b). After 4000 cycles, 41% of the initial ECA of the PIM@Pt/C (21.6 m^2 g^{-1}) remains while only 16% of the initial ECA remains for the Pt/C (8.6 m^2 g^{-1}) (Figure 3e). The ORR mass activity (0.791 V vs. NHE) for PIM@Pt/C (35% retention, 56.4 A g^{-1} Pt) also remains much higher than that for Pt/C (5% retention, 9 A g^{-1} Pt) after 4000 cycles.

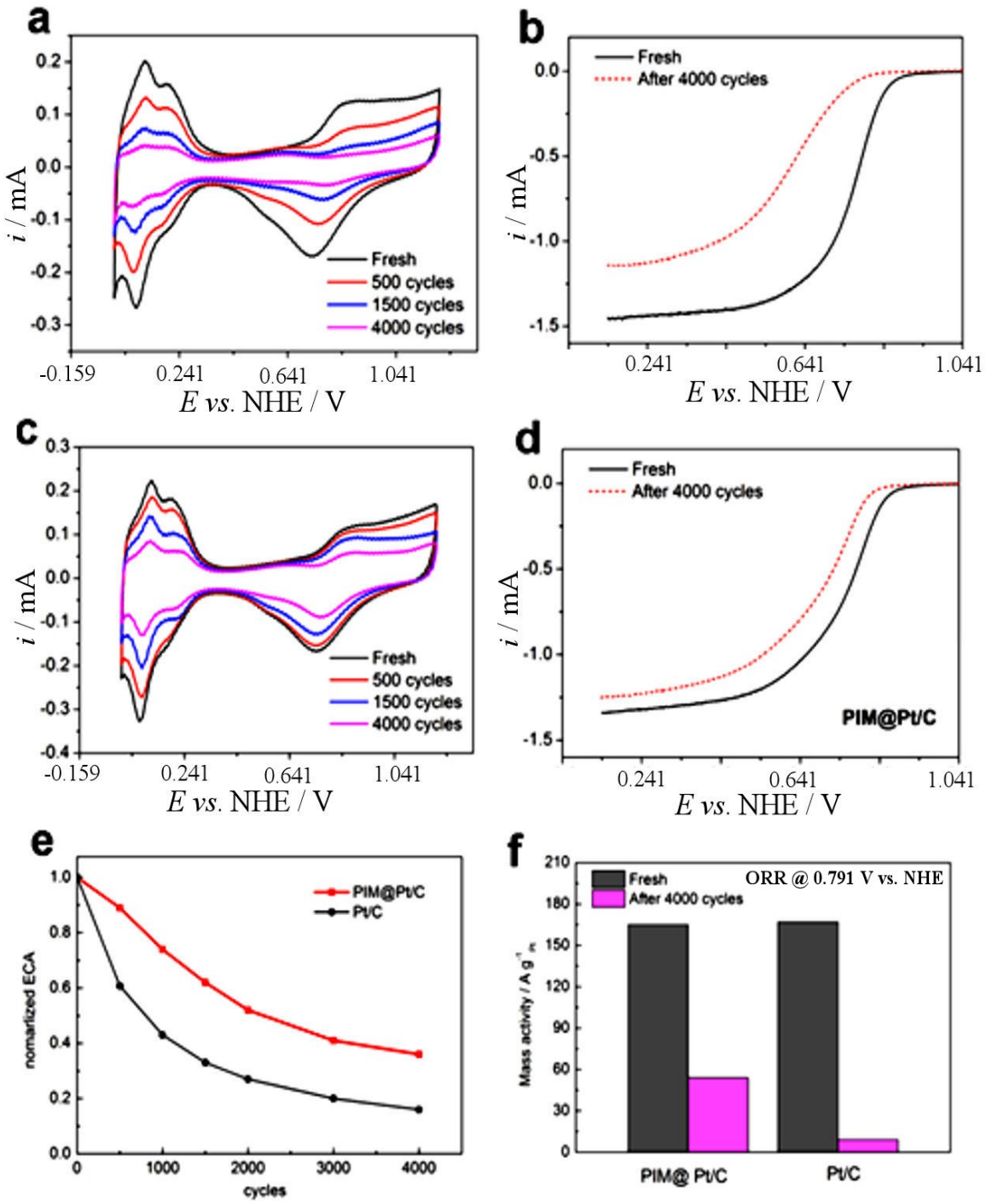

Figure 3. (a-d) CV curves and ORR polarization curves for Pt/C (a, b) and PIM@Pt/C (c, d) by ADT cycling from 0.541 to 1.141 V vs. NHE, (e) ECA loss rate and (f) ORR kinetic currents after 4000 cycles accelerated corrosion test.

The particle size distribution for Pt nanoparticles is obtained from HRTEM images by measuring more than 200 particles in each sample. As shown in Figure 4a and 4c, both the PIM@Pt/C and Pt/C catalysts show some degree of corrosion after 4000 CV cycles. However, the Pt/C shows a higher degree corrosion than PIM@Pt/C. Pt nanoparticle aggregation and carbon support corrosion can be found almost everywhere in the Pt/C catalyst (Figure 4c) with the mean particle size of the Pt/C increasing from 3.0 nm the initial diameter to 9.2 nm after 4000 CV cycles (Figure 4d), which is indicative of severe aggregation of Pt NPs for the Pt/C catalyst. Aggregation also occurs to Pt nanoparticles for PIM@Pt/C (Figure 4a), but to a much lesser extent. The mean size of Pt particles is only 5.6 nm (Figure 4b). The accelerated corrosion test and TEM results show that the protection of PIM-EA-TB endows the Pt/C catalyst with high stabilization, effectively preventing the Pt NPs aggregation with each other and preventing the Pt loss by catalyst support corrosion. This is critical for the long-term performance of PEM fuel cells.

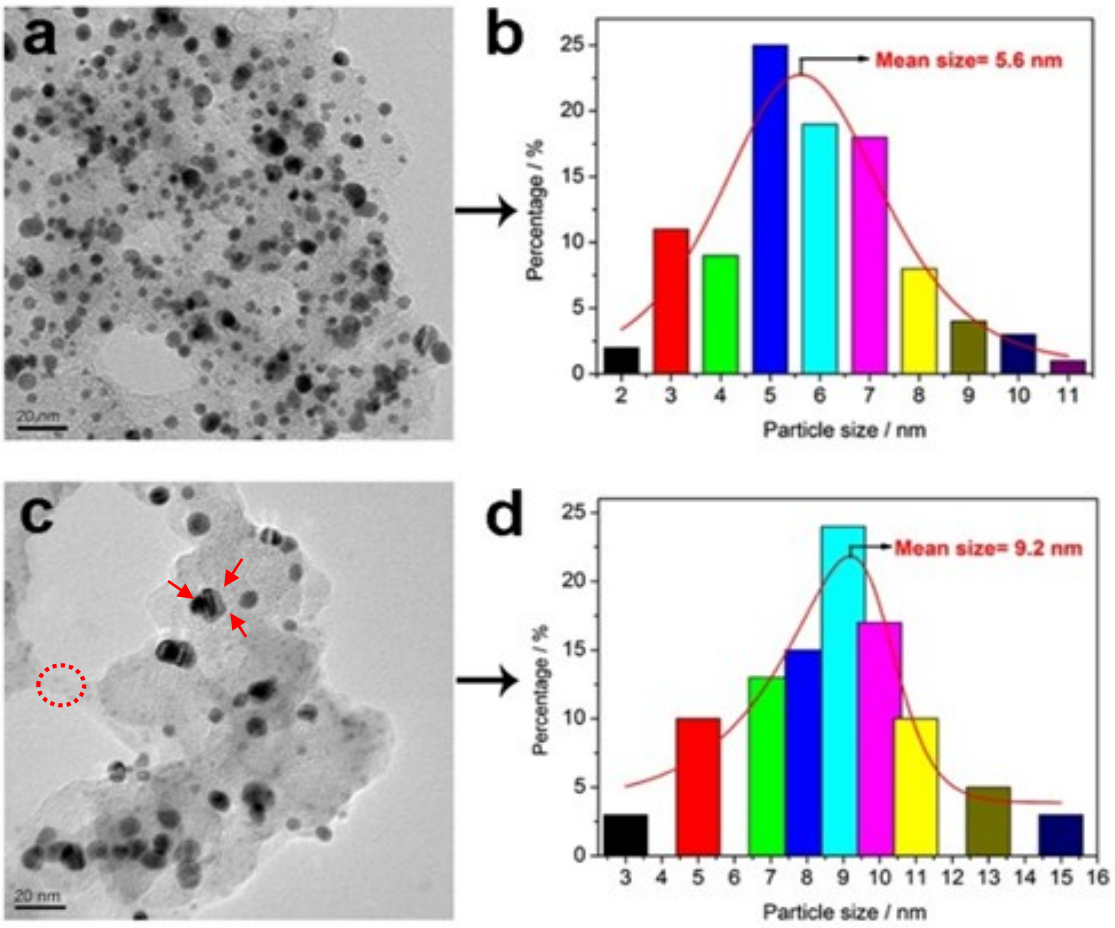

Figure 4. TEM images and size distribution of Pt nanoparticles for PIM@Pt/C (a, b) and Pt/C (c, d) after ADT test.

4. Conclusion

A new strategy is proposed to design stable fuel cell electrocatalysts by coating with novel highly rigid and microporous PIM materials such as PIM-EA-TB. The rigid PIM matrix leads to a more stable Pt/C catalyst surface, whilst maintaining a high rate of transport for reagents and products. Significantly, the PIM protection can effectively prevent the Pt nanoparticles from migrating/aggregating and suppress Pt loss by catalyst support corrosion. Further improvements with PIM structure optimisation are likely.

Acknowledgement

D.H. thanks the Royal Society for a Newton International Fellowship. F.M. thanks Dr. Robert Potter from Johnson–Matthey for support with catalyst materials and for helpful discussion.

References

[1] N. Cheng, M.N. Banis, J. Liu, A. Riese, X. Li, R. Li, S. Ye, S. Knights, X. Sun, Extremely stable platinum nanoparticles encapsulated in a zirconia nanocage by area-selective atomic layer deposition for the oxygen reduction reaction, Adv. Mater. 27 (2015) 277-281.

[2] B.C.H. Steele, A. Heinzel, A. Heinzel, Materials for fuel-cell technologies, Nature 414 (2001) 345-352.

[3] N. Cheng, S. Mu, M. Pan, P.P. Edwards, Improved lifetime of PEM fuel cell catalysts through polymer stabilization, Electrochem. Commun. 11 (2009) 1610-1614.

[4] X. Yu, A. Manthiram, Catalyst-selective, scalable membraneless alkaline direct formate fuel cells, Appl. Catal. B 165 (2015) 63-67.

[5] J. Zhang, K. Sasaki, E. Sutter, R.R. Adzic, Stabilization of platinum oxygen-reduction electrocatalysts using gold clusters, Science 315 (2007) 220-222.

[6] E.G. Ciapina, S.F. Santos, E.R. Gonzalez, The electrooxidation of carbon monoxide on unsupported Pt agglomerates, J. Electroanal. Chem. 644 (2010) 132-143.

[7] S. Chen, Z. Wei, X. Qi, L. Dong, Y. Guo, L. Wan, Z. Shao, L. Li, Nanostructured polyaniline-decorated Pt/C@ PANI core-shell catalyst with enhanced durability and activity, J. Am. Chem. Soc. 134 (2012) 13252-13255.

[8] X. Yu, S. Ye, Recent advances in activity and durability enhancement of Pt/C catalytic cathode in PEMFC: Part II: Degradation mechanism and durability enhancement of carbon supported platinum catalyst, J. Power Sources 172 (2007) 145-154.

[9] Z. Chen, M. Waje, W. Li, Y. Yan, Supportless Pt and PtPd Nanotubes as electrocatalysts for oxygen-reduction reactions, Angew. Chem. Int. Ed. 46 (2007) 4060-4063.

[10] D. He, C. Zeng, C. Xu, N. Cheng, H. Li, S. Mu, M. Pan, Polyaniline-functionalized carbon nanotube supported platinum catalysts, Langmuir 27 (2011) 5582-5588.

[11] D. Wang, H. Xin, R. Hovden, H. Wang, Y. Yu, D.A. Muller, F.J. DiSalvo, H.D. Abruña, Structurally ordered intermetallic platinum-cobalt core-shell nanoparticles with enhanced activity and stability as oxygen reduction electrocatalysts, Nature Mater. 12 (2013) 81-87.

[12] P.M. Arnal, M. Comotti, F. Schüth, High-temperature-stable catalysts by hollow sphere encapsulation, Angew. Chem. 118 (2006) 8404-8407.

[13] P. Lu, C.T. Campbell, Y. Xia, A sinter-resistant catalytic system fabricated by maneuvering the selectivity of SiO2 deposition onto the TiO2 surface versus the Pt nanoparticle surface, Nano Lett. 13 (2013) 4957-4962.

[14] S.H. Lee, D.M. Hoffman, A.J. Jacobson, T.R. Lee, Transparent, Homogeneous tin oxide (SnO2) thin films containing SnO2-coated gold nanoparticles, Chem. Mater. 25 (2013) 4697-4702.

[15] S.V. Adymkanov, Y.P. Yampolskii, A.M. Polyakov, P.M. Budd, K.J. Reynolds, N.B. McKeown, K.J. Msayib, Pervaporation of alcohols through highly permeable PIM-1 polymer films, Polymer Science Ser. A 50 (2008) 444-450.

[16] C.G. Bezzu, M. Carta, A. Tonkins, J.C. Jansen, P. Bernardo, F. Bazzarelli, N.B. McKeown, A spirobifluorene-based polymer of intrinsic microporosity with improved performance for gas separation, Adv. Mater. 24 (2012) 5930-5933.

[17] E. Madrid, Y. Rong, M. Carta, N.B. McKeown, R.M. Evans, G.A. Attard, T.J. Clarke, S.H. Taylor, Y. Long, F. Marken, Metastable ionic diodes derived from an amine-based polymer of intrinsic microporosity, Angew. Chem. 40 (2014) 10927-10930.

[18] Y. Rong, R.M. Evans, M. Carta, N.B. McKeown, G.A. Attard, F. Marken, Intrinsically porous polymer protects catalytic gold particles for enzymeless glucose oxidation, Electroanalysis 26 (2014) 904-909.

[19] Y. Rong, R.M. Evans, M. Carta, N.B. McKeown, G.A. Attard, F. Marken, High density heterogenisation of molecular electrocatalysts in a rigid intrinsically microporous polymer host, Electrochem. Commun. 46 (2014) 26-29.

[20] M. Carta, R.M. Evans, M. Croad, Y. Rogan, J.C. Jansen, P. Bernardo, F. Bazzarelli, N. B. McKeown, An efficient polymer molecular sieve for membrane gas separations, Science 339 (2013) 303-307.

[21] D. He, S. Mu, M. Pan, Perfluorosulfonic acid-functionalized Pt/carbon nanotube catalysts with enhanced stability and performance for use in proton exchange membrane fuel cells, Carbon 49 (2011) 82-88.

[22] B. Lim, M. Jiang, P.H.C. Camargo, E.C. Cho, J. Tao, X. Lu, Y. Zhu, Y. Xia, Pd-Pt bimetallic nanodendrites with high activity for oxygen reduction, Science 324 (2009) 1302-1305.